

## Modeling and Simulation of Bacterial Self-Organization in Circular Container Along Contact Line as Detected by Bioluminescence Imaging

Romas Baronas, Žilvinas Ledas  
 Faculty of Mathematics and Informatics  
 Vilnius University  
 Naugarduko 24, LT-03225 Vilnius, Lithuania  
 Emails: romas.baronas@mif.vu.lt, zilvinas.ledas@mif.vu.lt

Remigijus Šimkus  
 Institute of Biochemistry  
 Vilnius University  
 Mokslininku 12, LT-08662 Vilnius, Lithuania  
 Email: remigijus.simkus@bchi.vu.lt

**Abstract**—Mathematical modeling and numerical simulation of quasi-one dimensional spatiotemporal pattern formation along the three phase contact line in the fluid cultures of lux-gene engineered *Escherichia coli* is investigated in this paper. The numerical simulation is based on a one-dimensional-in-space mathematical model of a bacterial self-organization as detected by quasi-one-dimensional bioluminescence imaging. The pattern formation in a luminous *E. coli* colony was mathematically modeled by the nonlinear reaction-diffusion-chemotaxis equations. The numerical simulation was carried out using the finite difference technique. Regular oscillations as well as chaotic fluctuations similar to the experimental ones were computationally simulated. The influence of the signal-dependent as well as density-dependent chemotactic sensitivity, the non-local sampling and the diffusion nonlinearity on the pattern formation was investigated. The computational simulations showed that a constant chemotactic sensitivity, a local sampling and a linear diffusion can be applied for modeling the formation of the bioluminescence patterns in a colony of luminous *E. coli*.

**Keywords**—chemotaxis; reaction-diffusion; pattern formation; simulation; whole-cell biosensor.

### I. INTRODUCTION

This paper is an extension of work originally reported in The Third International Conference on Advances in System Simulation [1].

Various microorganisms respond to certain chemicals found in their environment by migrating towards higher (chemoattraction) or lower (chemorepulsion) concentrations of the substance. The directed movement of microorganisms in response to chemical gradients is called chemotaxis [2]. Chemotaxis plays a crucial role in a wide range of biological phenomena, e.g., within the embryo, the chemotaxis affects avian gastrulation and patterning of the nervous system [3]. Often, microorganisms not only move up chemical gradients towards a chemoattractant, but they are also able to produce more of the chemoattractant. This is the effect that produces the aggregation of the motile microorganisms into local clusters with high density and hence results in a pattern formation [4].

Although the chemotaxis has been observed in many bacterial species, *Escherichia coli* is one of the mostly

studied examples. *E. coli* responds to the chemical stimulus by alternating the rotational direction of their flagella [2], [3].

Various mathematical models based on the Patlak-Keller-Segel model have been successfully used as important tools to study the mechanisms of the chemotaxis [5]. An excellent review on the mathematical modeling of the chemotaxis has been presented by Hillen and Painter [6].

Bacterial species including *E. coli* have been observed to form various patterns under different environmental conditions [4], [7], [8]. Bacterial populations are capable of self-organization into states exhibiting strong inhomogeneities in density [9], [10]. Recently, the spatiotemporal patterns in the fluid cultures of *E. coli* have been observed by employing lux-gene engineered cells and a bioluminescence imaging technique [11], [12]. However, the mechanisms governing the formation of bioluminescence patterns still remain unclear.

Over the last two decades, lux-gene engineered bacteria have been successfully used to develop whole cell-based biosensors [13]. A whole-cell biosensor is an analyte probe consisting of a biological element, such as a genetically engineered bacteria, integrated with an electronic component to yield a measurable signal [14]. Whole-cell biosensors have been successfully used for the detection of environmental pollutant bioavailability, various stressors, including dioxins, endocrine-disrupting chemicals, and ionizing radiation [15]. To solve the problems currently limiting the practical use of whole-cell biosensors, the bacterial self-organization within the biosensors have to be comprehensively investigated.

In this paper, the bacterial self-organization in a small circular container near the three phase contact line is investigated [11], [12]. A computational model for efficient simulating the formation of the spatiotemporal patterns experimentally detected by quasi-one-dimensional bioluminescence imaging in the fluid cultures of *E. coli* has recently been developed [16], [17]. The pattern formation in a luminous *E. coli* colony was modeled by the nonlinear reaction-diffusion-chemotaxis equations. The mathematical model was formulated in a one-dimensional space. Several

different model variations were analyzed, and a minimal model was obtained for simulating the formation of the bioluminescence patterns representing the self-organization of luminous *E. coli*.

The aim of this work was to improve the already existing computational model by introducing the nonlinear diffusion of cells, the non-local sampling and several kinds of the chemotactic sensitivity [6]. By extending the model in this way, the improvements of the patterns simulated using extended model were expected. In this paper, the pattern formation is computationally investigated assuming two kinds of the chemotactic sensitivity, the signal-dependent sensitivity and the density-dependent sensitivity. The non-local sampling and the nonlinear diffusion are investigated individually and collectively. The numerical simulation at transient conditions was carried out using the finite difference technique [18]. The computational model was validated by experimental data. Regular oscillations as well as chaotic fluctuations similar to experimental ones were computationally simulated. By varying the input parameters the output results were analyzed with a special emphasis on the influence of the model parameters on the spatiotemporal pattern formation in the luminous *E. coli* colony.

The rest of the paper is organized as follows. Section II provides a state of the art on the mathematical modeling of bacterial self-organization. Section III describes the mathematical model of the bacterial self-organization in a circular container. The computational modeling of a physical experiment is discussed in Section IV. Section V is devoted to the results of the numerical simulation where the effects of different chemotactic sensitivity functions, the non-local gradient and the diffusion nonlinearity are investigated. Finally, the main conclusions are summarized in Section VI.

## II. MODELS OF BACTERIAL SELF-ORGANIZATION

Different mathematical models based on advection-reaction-diffusion equations have already been developed for computational modeling the pattern formation in bacterial colonies [7], [8], [19], [20], [21]. The system of coupled nonlinear partial differential equations introduced by Keller and Segel are still among the most widely used [5], [6].

According to the Keller and Segel approach, the main biological processes can be described by a system of two conservation equations ( $x \in \Omega$ ,  $t > 0$ ),

$$\begin{aligned} \frac{\partial n}{\partial t} &= \nabla (D_n \nabla n - h(n, c)n \nabla c) + f(n, c), \\ \frac{\partial c}{\partial t} &= \nabla (D_c \nabla c) + g_p(n, c)n - g_d(n, c)c, \end{aligned} \quad (1)$$

where  $x$  and  $t$  stand for space and time,  $n(x, t)$  is the cell density,  $c(x, t)$  is the chemoattractant concentration,  $D_n(n)$  and  $D_c$  are the diffusion coefficients,  $f(n, c)$  stands for cell

growth and death,  $h(n, c)$  stands for the chemotactic sensitivity,  $g_p$  and  $g_d$  describe the production and degradation of the chemoattractant [5], [21].

Both diffusion coefficients,  $D_n$  and  $D_c$ , are usually assumed to be constant. However, the nonlinear cell diffusion depending on the chemoattractant concentration or/and the cell density is also considered [6]. In this work, we consider the nonlinear diffusion of the form

$$D_n(n) = D_n \left( \frac{n}{n_0} \right)^m, \quad (2)$$

where and below  $n_0$  is the maximal density ("carrying capacity") of the cell population ( $n < n_0$ ) [22]. At  $m < 0$  the rate of diffusion increases with increasing the cell density, while at  $m > 0$  the rate decreases with increasing the cell density. Accepting  $m = 0$  leads to a constant rate of the cell diffusion. Since the proper form of the diffusion coefficient  $D_n$  to be used for the simulation of the spatiotemporal pattern formation in the fluid cultures of lux-gene engineered *E. coli* is unknown, the simulation was performed at different values of  $m$ .

The cell growth  $f(n, c)$  is usually assumed to be a logistic function,

$$f(n, c) = k_1 n \left( 1 - \frac{n}{n_0} \right), \quad (3)$$

where  $k_1$  is the constant growth rate of the cell population [7].

Various chemoattractant production functions have been used in chemotactic models [6]. Usually, a saturating function of the cell density is used indicating that, as the cell density increases, the chemoattractant production decreases. The Michaelis-Menten function is widely used to express the production rate  $g_p$  [5], [20], [23],

$$g_p(n, c) = \frac{k_2}{k_3 + n}. \quad (4)$$

The degradation or consumption  $g_d$  of the chemoattractant is typically constant,

$$g_d(n, c) = k_4. \quad (5)$$

Values of  $k_2$ ,  $k_3$  and  $k_4$  are not exactly known yet [21].

The function  $h(n, c)$  controls the chemotactic response of the cells to the chemoattractant. The signal-dependent sensitivity and the density-dependent sensitivity are two main kinds of the chemotactic sensitivity  $h(n, c)$  [6]. In order to reproduce the experimentally observed bands Keller and Segel introduced a chemotactic (signal-dependent) sensitivity of the following form [24]:

$$h(n, c) = \frac{k_5}{c}. \quad (6)$$

Since the bacterial current flow declines at low chemical concentrations and saturates at high concentrations, Lapidus and Schiller derived the "receptor" chemotactic (signal-dependent) sensitivity for *E. coli* [19],

$$h(n, c) = \frac{k_6}{(k_7 + c)^2}. \quad (7)$$

Assuming that cells carry a certain finite volume, a density-dependent chemotactic sensitivity function as well as volume-filling model were derived by Hillen and Painter [25],

$$h(n, c) = k_8 \left(1 - \frac{n}{n_0}\right). \quad (8)$$

Another form for the density-dependent chemotactic sensitivity has been introduced by Velazquez [26],

$$h(n, c) = \frac{k_9}{k_{10} + n}. \quad (9)$$

In the simplest form, the chemotactic sensitivity is assumed to be independent of the chemoattractant concentration  $c$  as well as the cell density  $n$ , i.e.,  $h(n, c)$  is constant,  $h(n, c) = k_8$ . Since the proper form of the chemotactic sensitivity function  $h(n, c)$  to be used for the simulation of the spatiotemporal pattern formation in the fluid cultures of lux-gene engineered *E. coli* remains unknown, all these four forms of the function  $h(n, c)$  were used to find out the most useful form.

*E. coli* is able to detect a gradient by sampling the chemoattractant concentration over the time and adjusting their movement accordingly. As a result, the signal detected by the cell is non-local and the non-local gradient can be used to model this behaviour [27], [28],

$$\overset{\circ}{\nabla}_\rho c(x, t) = \frac{n}{|S^{n-1}| \rho} \int_{S^{n-1}} \sigma c(x + \rho \sigma, t) d\sigma, \quad (10)$$

where  $S^{n-1}$  denotes the  $(n-1)$ -dimensional unit sphere in  $\mathbb{R}^n$  and  $\rho$  is the sampling radius. When  $\rho \rightarrow 0$ , this model collapses to the ordinary model with local sampling.

It was recently shown that the Keller-Segel approach can be applied to the simulation of the formation of the spatiotemporal patterns experimentally detected by bioluminescence imaging in the fluid cultures of *E. coli* [16], [17]. This work aims to improve the already existing computational model by introducing the nonlinear diffusion (2) of cells, the non-local sampling (10) and different kinds of the chemotactic sensitivity (6)-(9). The improvement of the patterns simulated using the extended model was expected.

### III. MODEL FOR LUMINOUS *E. Coli*

When modeling the self-organization of luminous *E. Coli* in a circular container along the three phase contact line [11], [12], the mathematical model can be defined in one spatial dimension - on the circumference of the vessel [16], [17].

#### A. Governing Equations

Replacing  $f$ ,  $g_p$ ,  $g_d$ ,  $D_n$  and  $\nabla c$  with the concrete expressions above, the governing equations (1) reduce to a cell kinetics model with the nonlinear signal kinetics, the nonlinear cell diffusion, the nonlinear chemotactic sensitivity and the non-local sampling,

$$\frac{\partial n}{\partial t} = D_n \nabla \left( \left( \frac{n}{n_0} \right)^m \nabla n \right) - \nabla \left( h(n, c) n \overset{\circ}{\nabla}_\rho c \right) + k_1 n \left( 1 - \frac{n}{n_0} \right), \quad (11)$$

$$\frac{\partial c}{\partial t} = D_c \Delta c + \frac{k_2 n}{k_3 + n} - k_4 c, \quad x \in (0, l), \quad t > 0,$$

where  $\Delta$  is the Laplace operator formulated in the one-dimensional Cartesian coordinate system, and  $l$  is the length of the contact line, i.e., the circumference of the vessel. Assuming  $R$  as the vessel radius,  $l = 2\pi R$ ,  $x \in (0, 2\pi R)$ .

#### B. Initial and Boundary Conditions

A non-uniform initial distribution of cells and zero concentration of the chemoattractant are assumed,

$$\begin{aligned} n(x, 0) &= n_{0x}(x), \\ c(x, 0) &= 0, \quad x \in [0, l], \end{aligned} \quad (12)$$

where  $n_{0x}(x)$  stands for the initial ( $t = 0$ ) spatially-varying cell density.

For the bacterial simulation on a continuous circle of the length  $l$  of the circumference, the following periodicity conditions are applied as the boundary (matching) conditions ( $t > 0$ ):

$$\begin{aligned} n(0, t) &= n(l, t), \quad \frac{\partial n}{\partial x} \Big|_{x=0} = \frac{\partial n}{\partial x} \Big|_{x=l}, \\ c(0, t) &= c(l, t), \quad \frac{\partial c}{\partial x} \Big|_{x=0} = \frac{\partial c}{\partial x} \Big|_{x=l}. \end{aligned} \quad (13)$$

#### C. Dimensionless Model

In order to define the main governing parameters of the mathematical model (11)-(13), a dimensionless mathematical model has been derived by introducing the following dimensionless parameters [4], [6], [23]:

$$\begin{aligned} u &= \frac{n}{n_0}, \quad v = \frac{k_3 k_4 c}{k_2 n_0}, \\ t^* &= \frac{k_4 t}{s}, \quad x^* = \sqrt{\frac{k_4}{D_c s}} x, \\ D &= \frac{D_n}{D_c}, \quad r = \frac{k_1}{k_4}, \quad \phi = \frac{n_0}{k_3}, \quad \rho^* = \frac{\rho}{l}, \\ \chi(u, v) &= \frac{k_2 n_0}{k_3 k_4 D_c} h(n_0 u, k_2 n_0 c / (k_3 k_4)). \end{aligned} \quad (14)$$

Dropping the asterisks, the dimensionless governing equations then become ( $t > 0$ )

$$\begin{aligned}\frac{\partial u}{\partial t} &= \frac{\partial}{\partial x} \left( Du^m \frac{\partial u}{\partial x} \right) - \frac{\partial}{\partial x} \left( \chi(u, v) u \overset{\circ}{\nabla}_\rho v \right) + \\ &\quad + sru(1 - u), \\ \frac{\partial v}{\partial t} &= \frac{\partial^2 v}{\partial x^2} + s \left( \frac{u}{1 + \phi u} - v \right), \quad x \in (0, 1),\end{aligned}\quad (15)$$

where  $x$  and  $t$  stand for the dimensionless space and time, respectively,  $u$  is the dimensionless cell density,  $v$  is the dimensionless chemoattractant concentration,  $r$  is the dimensionless growth rate of the cell population,  $\phi$  stands for saturating of the signal production,  $\chi(u, v)$  is the dimensionless chemotactic sensitivity, and  $s$  stands for the spatial and temporal scale.

Assuming the one-dimensional Cartesian coordinate system the non-local gradient can be described as

$$\overset{\circ}{\nabla}_\rho v(x, t) = \frac{v(x + \rho, t) - v(x - \rho, t)}{2\rho}. \quad (16)$$

For the dimensionless simulation of the spatiotemporal pattern formation in a luminous *E. coli* colony, four forms of the chemotactic sensitivity function  $\chi(u, v)$  were used to find out the best fitting pattern for the experimental data [11], [12], [16],

$$\chi(u, v) = \frac{\chi_0}{(1 + \alpha v)^2}, \quad (17a)$$

$$\chi(u, v) = \chi_0 \frac{1 + \beta}{v + \beta}, \quad (17b)$$

$$\chi(u, v) = \chi_0 \left( 1 - \frac{u}{\gamma} \right), \quad (17c)$$

$$\chi(u, v) = \frac{\chi_0}{1 + \epsilon u}. \quad (17d)$$

The first two forms (17a) and (17b) of the function  $\chi(u, v)$  correspond to the signal-dependent sensitivity, while the other two (17c) and (17d) - for the density-dependent sensitivity [6]. Accepting  $\alpha = 0$ ,  $\beta \rightarrow \infty$ ,  $\gamma \rightarrow \infty$  or  $\epsilon = 0$  leads to a constant form of the chemotactic sensitivity,  $\chi(u, v) = \chi_0$ .

The initial conditions (12) take the following dimensionless form:

$$\begin{aligned}u(x, 0) &= 1 + \varepsilon(x), \\ v(x, 0) &= 0, \quad x \in [0, 1],\end{aligned}\quad (18)$$

where  $\varepsilon(x)$  is a random spatial perturbation.

The boundary conditions (13) transform to the following dimensionless equations ( $t > 0$ ):

$$\begin{aligned}u(0, t) &= u(1, t), \quad \frac{\partial u}{\partial x} \Big|_{x=0} = \frac{\partial u}{\partial x} \Big|_{x=1}, \\ v(0, t) &= c(1, t), \quad \frac{\partial v}{\partial x} \Big|_{x=0} = \frac{\partial v}{\partial x} \Big|_{x=1}.\end{aligned}\quad (19)$$

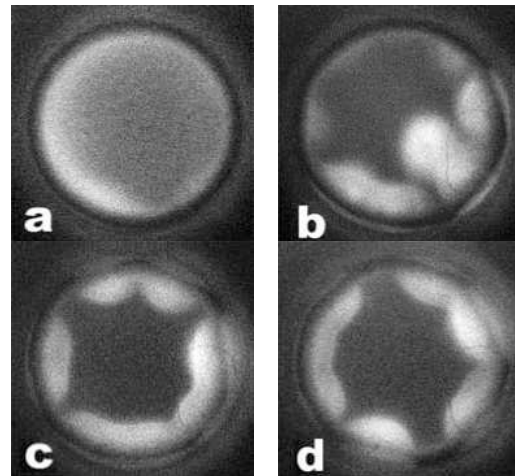


Figure 1. Top view bioluminescence images of the bacterial cultures in the cylindrical glass vessel. The images were captured at 5 (a), 20 (b), 40 (c), 60 (d) min [12].

According to the classification of chemotaxis models, the dimensionless model of the pattern formation is a combination of the signal-dependent sensitivity (M2), the density-dependent sensitivity (M3), the non-local sampling (M4), the nonlinear diffusion (M5), the saturating signal production (M6) and the cell kinetics (M8) models [6]. At certain values of the model parameters the dimensionless model (15), (18) and (19) reduces to the minimal model (M1) for the chemotaxis [6].

#### IV. NUMERICAL SIMULATION

The mathematical model (11)-(13), as well as the corresponding dimensionless model (15), (18), (19), has been defined as an initial boundary value problem based on a system of nonlinear partial differential equations. No analytical solution is possible because of the nonlinearity of the governing equations of the model [4]. Hence the bacterial self-organization was simulated numerically.

The numerical simulation was carried out using the finite difference technique [18]. To find a numerical solution of the problem a uniform discrete grid with 760 points and the dimensionless step size  $1/760$  (dimensionless units) in the space direction was introduced,  $760 \times 1/760 = 1$ . A constant dimensionless step size  $2.5 \times 10^{-7}$  was also used in the time direction. An explicit finite difference scheme has been built as a result of the difference approximation [17], [18], [29], [30]. The digital simulator has been programmed by the authors in Free Pascal language [31].

The computational model was applied to the simulation of bioluminescence patterns observed in a small circular containers made of glass [12], [16]. Figure 1 shows typical top view bioluminescence images of bacterial cultures illustrating an accumulation of luminous bacteria near the

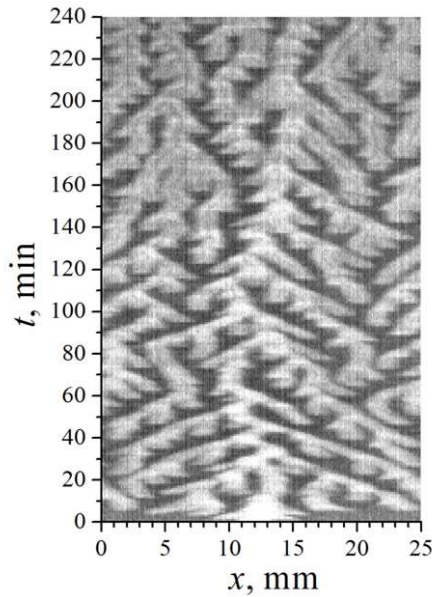


Figure 2. Space-time plot of bioluminescence measured along the contact line of the cylindrical vessel [12], [16].

contact line. The images were captured at different times of the population evolution.

In general, the dynamic processes in unstirred cultures are rather complicated and need to be modeled in three dimensional space [2], [11], [12]. Since luminous cells concentrate near the contact line, the three-dimensional processes were simulated in one dimension (quasi-one dimensional rings in Figure 1). Figure 2 shows the corresponding space-time plot of quasi-one-dimensional bioluminescence intensity.

By varying the model parameters the simulation results were analyzed with a special emphasis to achieving a spatiotemporal pattern similar to the experimentally obtained pattern shown in Figure 2. Figure 3 shows the results of the informal pattern fitting, where Figures 3a and 3b present the simulated space-time plots of the dimensionless cell density  $u$  and the chemoattractant concentration  $v$ , respectively. The corresponding values  $\bar{u}$  and  $\bar{v}$  averaged on the circumference of the vessel are depicted in Figure 3c,

$$\begin{aligned}\bar{u}(t) &= \int_0^1 u(x, t) dx, \\ \bar{v}(t) &= \int_0^1 v(x, t) dx.\end{aligned}\quad (20)$$

Regular oscillations as well as chaotic fluctuations similar to the experimental ones were computationally simulated. Accepting the constant form of the chemotactic sensitivity ( $\chi(u, v) = \chi_0$ ) and the simple gradient, the dynamics of the bacterial population was simulated at the following values of the model parameters [16]:

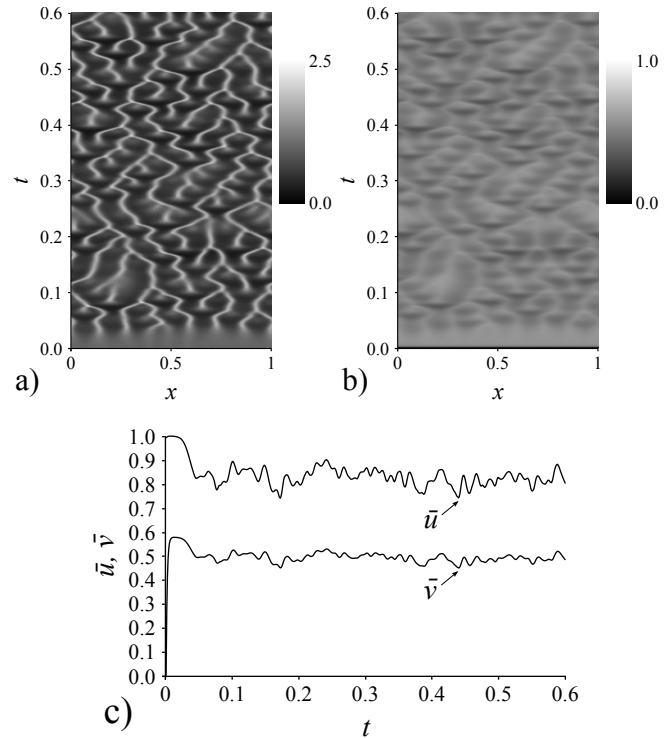


Figure 3. Simulated space-time plots of the dimensionless cell density  $u$  (a) as well as the chemoattractant concentration  $v$  (b) and the dynamics of the corresponding averaged values  $\bar{u}$  and  $\bar{v}$  (c). Values of the parameters are as defined in (21).

$$\begin{aligned}D &= 0.1, & \chi_0 &= 6.2, & \rho &= 0, & r &= 1, \\ \phi &= 0.73, & s &= 625, & m &= 0.\end{aligned}\quad (21)$$

A spatially-varying random perturbation  $\varepsilon(x)$  of the dimensionless cell density  $u$  of 10% was applied for the initial distribution of bacteria near the three phase contact line when simulating the spatiotemporal patterns.

Due to a relatively great number of model parameters, there is no guarantee that the values (21) mostly approach the pattern shown in Figure 2. Similar patterns were achieved at different values of the model parameters. The linearization and the stability analysis of homogenous solutions of the Keller-Segel model showed similar effects [32], [33]. An increase in one parameter can be often compensated by decreasing or increasing another one. Because of this, it is important to investigate the influence of the model parameters on the pattern formation and to develop a mathematical model containing a minimal number of parameters and ensuring a qualitative analysis of bacterial pattern formation in a liquid medium [6], [10], [17], [21].

## V. RESULTS AND DISCUSSION

By varying the input parameters the output results were analyzed with a special emphasis on the influence of the

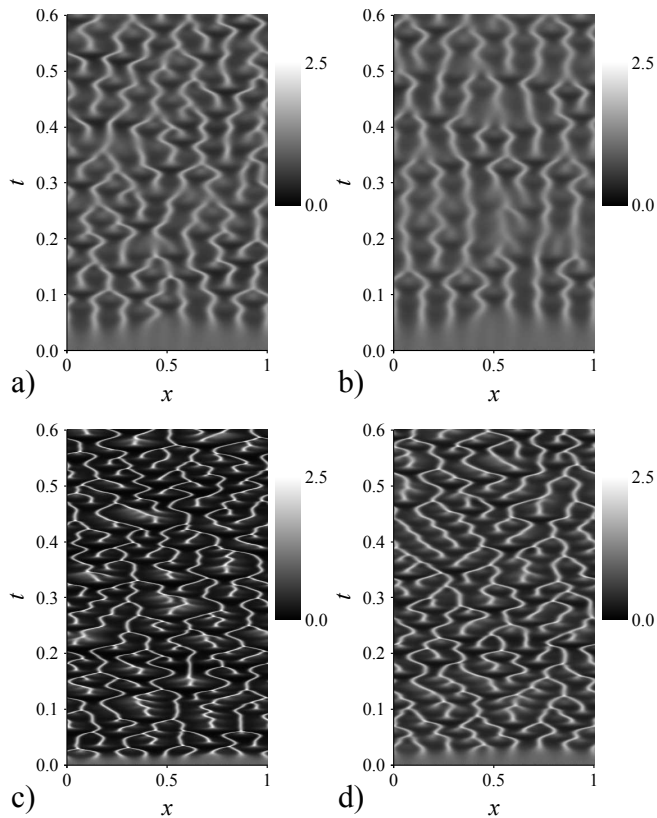


Figure 4. Spatiotemporal plots of the dimensionless cell density  $u$  for two forms of the signal-dependent chemotactic sensitivity  $\chi(u, v)$ : (17a) ( $\alpha = 0.05$ ) (a), ( $\alpha = 0.07$ ) (b) and (17b) ( $\beta = 2$ ) (c), ( $\beta = 10$ ) (d). Values of the other parameters are as defined in (21).

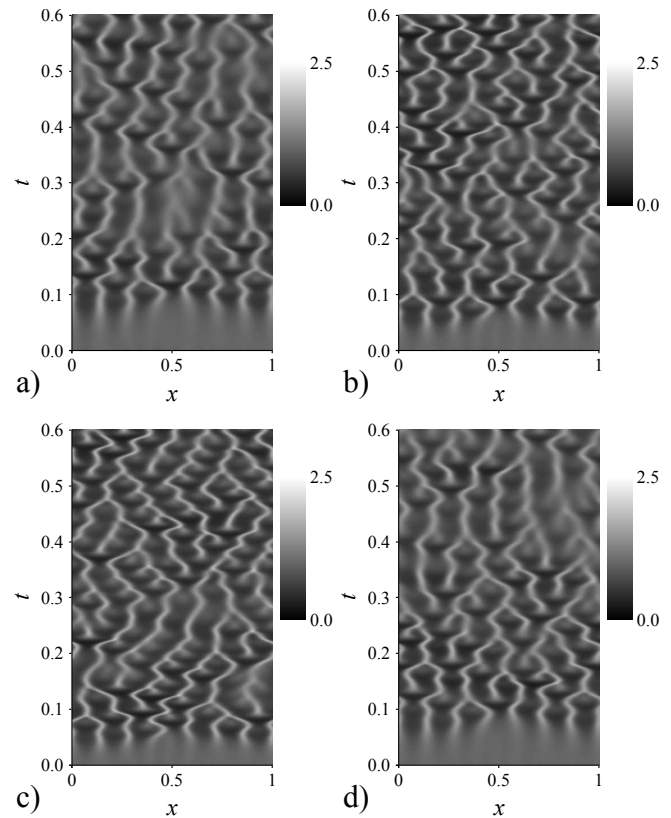


Figure 5. Spatiotemporal plots of the dimensionless cell density  $u$  for two forms of the density-dependent chemotactic sensitivity  $\chi(u, v)$ : (17c) ( $\gamma = 10$ ) (a), ( $\gamma = 15$ ) (b) and (17d) ( $\epsilon = 0.05$ ) (c), ( $\epsilon = 0.1$ ) (d). Values of the other parameters are as defined in (21).

chemotactic sensitivity, the non-local gradient and the diffusion nonlinearity on the spatiotemporal pattern formation in the luminous *E. coli* colony. Figure 3a shows the spatiotemporal pattern for the constant form of the chemotactic sensitivity ( $\chi(u, v) = \chi_0$ ) applying the simple gradient ( $\rho = 0$ ) and the linear diffusion ( $m = 0$ ).

The effects of the different chemotactic sensitivity functions were investigated assuming the linear diffusion ( $m = 0$ ) and the simple gradient ( $\rho \rightarrow 0$ ). The non-local gradient and the nonlinear diffusion was analyzed separately and together assuming the constant chemotactic sensitivity.

#### A. The Effect of the Signal-Dependent Sensitivity

The signal-dependent sensitivity was computationally modeled by two forms of the chemotactic sensitivity function  $\chi(u, v)$ : (17a) and (17b). The spatiotemporal patterns of the dimensionless cell density  $u$  were simulated at very different values of  $\alpha$  and  $\beta$ . Figure 4 shows the effect of the signal-dependence of the chemotactic sensitivity on the pattern formation.

Accepting  $\alpha = 0$  or  $\beta \rightarrow \infty$  leads to a signal-independence, i.e., a constant form, of the chemotactic sensitivity,  $\chi(u, v) = \chi_0$ . Results of the multiple simulations

showed that the simulated patterns distinguish from the experimental one (Figure 2) when increasing  $\alpha$ -parameter (Figures 4a and 4b) or decreasing  $\beta$ -parameter (Figures 4c and 4d). Because of this, there is no practical reason for application of a non-constant form of the signal-dependent sensitivity to modeling the formation of the bioluminescence patterns in a colony of luminous *E. coli*. Consequently, the signal-dependence of the chemotactic sensitivity can be ignored when modeling the pattern formation in the luminous *E. coli* colony.

#### B. The Effect of the Density-Dependent Sensitivity

Two forms, (17c) and (17d), of the chemotactic sensitivity function  $\chi(u, v)$  were employed for computational modeling of the density-dependent chemotactic sensitivity. The spatiotemporal patterns of the cell density  $u$  were simulated at various values of  $\gamma$  and  $\epsilon$ . Figure 5 shows how the density-dependence affects the pattern formation.

Accepting  $\gamma \rightarrow \infty$  or  $\epsilon = 0$  leads to a density-independence, i.e., a constant form, of the chemotactic sensitivity,  $\chi(u, v) = \chi_0$ . Multiple simulation showed that the simulated patterns distinguish from the experimental one (Figure 2) when decreasing  $\gamma$ -parameter (Figures 5a and 5b)

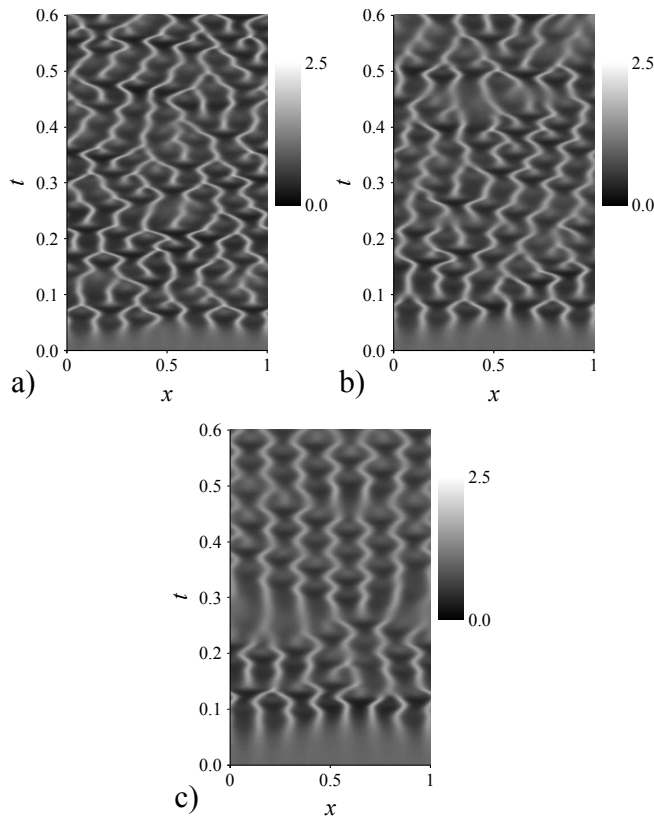


Figure 6. Spatiotemporal plots of the dimensionless cell density  $u$  when using the non-local sampling ( $\rho = 0.008$ ) (a), ( $\rho = 0.012$ ) (b), ( $\rho = 0.016$ ) (c). Values of the other parameters are as defined in (21).

or increasing  $\epsilon$ -parameter (Figures 5c and 5d). Because of this, similarly to the signal-dependent chemotactic sensitivity, there is no practical reason for application of a non-constant form also of the density-dependent sensitivity when modeling the pattern formation in a colony of luminous *E. coli*.

A simple constant form ( $\chi(u, v) = \chi_0$ ) of the chemotactic sensitivity can be successfully applied to modeling the formation of the bioluminescence patterns in a colony of luminous *E. coli*. Oscillations and fluctuations similar to experimental ones can be computationally simulated ignoring the signal-dependence as well as the density-dependence of the chemotactic sensitivity.

### C. The Effect of the Non-Local Sampling

The non-local sampling was modeled by using non-local gradient (16). The constant chemotactic sensitivity ( $\chi(u, v) = \chi_0$ ) was used in these simulations. The spatiotemporal patterns of the dimensionless cell density  $u$  were simulated at various values of the effective sampling radius  $\rho$ . Figure 6 shows how the non-local sampling affects the pattern formation in the luminous *E. coli* colony.

Accepting  $\rho = 0$  leads to a model with the local sampling

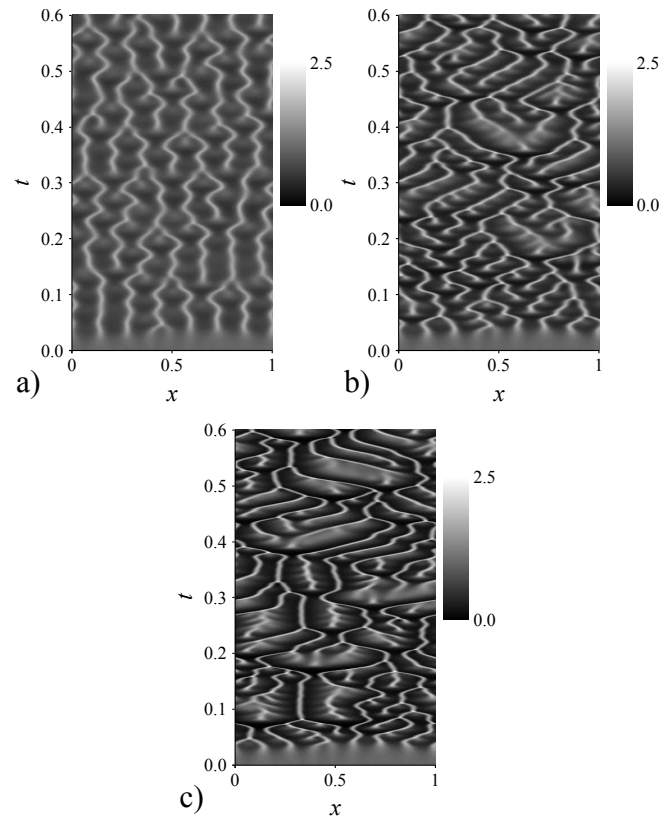


Figure 7. Spatiotemporal plots of the dimensionless cell density  $u$  when using the nonlinear diffusion ( $m = -0.6$ ) (a), ( $m = 0.2$ ) (b), ( $m = 0.6$ ) (c). Values of the other parameters are as defined in (21).

and the simple gradient, operator  $\overset{\circ}{\nabla}_\rho$  approaches  $\nabla$ . The computational results showed that the simulated patterns get dissimilar from the experimental one (Figure 2) when increasing  $\rho$ -parameter (Figure 6). As it can be seen from Figure 6c, merging of the different "branches" in the pattern is almost gone and this merging behaviour is essential to get patterns similar to experimental ones. Because of this, there is no practical reason for application of applying the non-local gradient to modeling the formation of the patterns in a colony of luminous *E. coli*.

### D. The Effect of the Nonlinear Diffusion

The nonlinear diffusion was modeled by using the following form of the diffusion function:  $D(u) = Du^m$  [22]. The chemotactic sensitivity was assumed to be constant ( $\chi(u, v) = \chi_0$ ) in these simulations. The spatiotemporal patterns of the dimensionless cell density  $u$  were simulated at various values of  $m$ -parameter. Figure 7 shows the effect of the nonlinearity of the diffusion.

Accepting  $m = 0$  leads to a model with the linear diffusion. Results of the simulations at different  $m$  values show that patterns tend to drift away from the experimental one (Figure 2) when increasing ( $m \rightarrow \infty$ ) (Figure 7c)

or decreasing ( $m \rightarrow -\infty$ ) (Figure 7a) the  $m$ -parameter. The pattern shown in Figure 7a contains less mergers of different "branches" (as a result of  $m \ll 0$ ). Figure 7 exhibits the "branch" movements that are distorted compared to the experimentally observed ones (as a result of  $m \gg 0$ ). Therefore, there is no need to use the nonlinear diffusion for modeling the pattern formation in a colony of luminous *E. coli*.

#### E. The Effect of the Non-Local Sampling With the Nonlinear Diffusion

From the simulations with the non-local gradient (the non-local sampling) and the nonlinear diffusion it was seen that the increasing the non-local gradient parameter  $\rho$  has visually opposite effect to the increasing nonlinear diffusion parameter  $m$  (Figure 6c versus Figure 7c). As a result, additional numerical experiments were carried out to determine how the non-local sampling combined with the nonlinear diffusion affects the pattern formation. Various combinations of  $\rho$ - and  $m$ -parameter values were used to simulate the spatiotemporal patterns of the dimensionless cell density  $u$  along the three phase contact line of the cylindrical vessel. Figure 8 shows the effects of the non-local sampling and the diffusion nonlinearity.

From Figure 8 it can be seen that the simulated patterns (especially Figure 8a) are more similar to the experimentally observed one (Figure 2) than those shown in Figures 6c and 7c. When analyzing the most distorted case (Figure 6c), one can see that the merging behaviour can be regained by using the nonlinear diffusion (Figures 8c and 8d), but the result is not quite similar to the desired one. However, if the nonlinear diffusion is added to the case shown in Figure 6b, the results (Figures 8a and 8b) become much better than those obtained considering the non-local sampling and the diffusion nonlinearity separately. This means that when increasing  $\rho$ , one should consider increasing  $m$ , respectively. On the other hand, the comparison of Figure 8a with Figure 3a does not confirm that the model with the non-local sampling and the nonlinear diffusion is capable to produce a result that better matches experimentally observed one. Because of this, there is no practical need for applying the non-local sampling as well as the nonlinear diffusion for the computational modeling of the pattern formation in a colony of luminous *E. coli*.

#### F. A minimal model

In the previous sections it was shown that the pattern formation along the contact line in a cellular population can be modeled at the following values of the model parameters:  $m = 0$ ,  $\alpha = 0$ ,  $\beta \rightarrow \infty$ ,  $\gamma \rightarrow \infty$ ,  $\epsilon = 0$ . The simulated patterns at these values tend to have the desired properties similar to the experimental ones (Figure 2) - emergence and merging of the strands are present and regular. Accepting

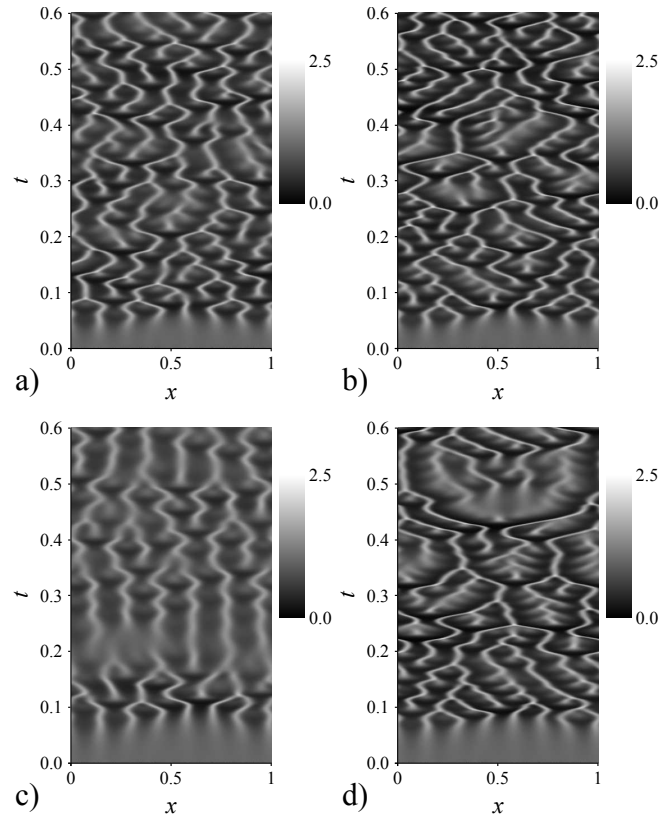


Figure 8. Spatiotemporal plots of the dimensionless cell density  $u$  when using the non-local sampling and the nonlinear diffusion ( $\rho = 0.012$ ,  $m = 0.2$ ) (a), ( $\rho = 0.012$ ,  $m = 0.4$ ) (b), ( $\rho = 0.016$ ,  $m = 0.2$ ) (c), ( $\rho = 0.016$ ,  $m = 0.6$ ) (d). Values of the other parameters are as defined in (21).

these values leads to a reduction of the governing equations (15) to the following form:

$$\begin{aligned} \frac{\partial u}{\partial t} &= D \frac{\partial^2 u}{\partial x^2} - \chi_0 \frac{\partial}{\partial x} \left( u \frac{\partial v}{\partial x} \right) + sru(1-u), \\ \frac{\partial v}{\partial t} &= \frac{\partial^2 v}{\partial x^2} + s \left( \frac{u}{1+\phi u} - v \right), \\ x &\in (0, 1), \quad t > 0. \end{aligned} \quad (22)$$

The governing equations (22), the initial (18) and the boundary (19) conditions form together a minimal mathematical model suitable for simulating the pattern formation in a colony of luminous *E. coli*.

According to the classification of the chemotaxis models introduced by Hillen and Painter [6], the minimal model (22) is a combination of two models: the nonlinear signal kinetics model M6 and the cell kinetics model M8. This combination of the models has comprehensively been analyzed by Maini and others [4], [20], [23].

The governing equations (22) contain five parameters,  $D$ ,  $\chi_0$ ,  $r$ ,  $\phi$  and  $s$ . The diffusion parameter  $D$  is necessary because of an inequality of the dimensional diffusion

coefficients  $D_n$  and  $D_c$  [4], [21]. The model parameter  $s$  is required to support the spatial and temporal scale for simulating systems and processes of the interest. The essential parameter  $\chi_0$  controls the chemotactic response of the cells to the concentrations of the attractant and allows to reproduce the experimentally observed bands. Earlier, it was shown that  $r$  and  $\phi$  are also essential for modeling the pattern formation in a colony of luminous *E. coli* [17].

## VI. CONCLUSIONS

The quasi-one dimensional spatiotemporal pattern formation along the three phase contact line in the fluid cultures of lux-gene engineered *Escherichia coli* can be simulated and studied on the basis of the Patlak-Keller-Segel model.

The mathematical model (11)-(13) and the corresponding dimensionless model (15), (18), (19) of the bacterial self-organization in a circular container as detected by bioluminescence imaging may be successfully used to investigate the pattern formation in a colony of luminous *E. coli*.

A constant function ( $\chi(u, v)$  as well as  $h(n, c)$ ) of the chemotactic sensitivity can be used for modeling the formation of the bioluminescence patterns in a colony of luminous *E. coli* (Figures 4 and 5). Oscillations and fluctuations similar to experimental ones (Figure 2) can be computationally simulated ignoring the signal-dependence as well as the density-dependence of the chemotactic sensitivity (Figure 3a).

The local sampling and the linear diffusion can be successfully applied to modeling the formation of the bioluminescence patterns in a colony of luminous *E. coli*. The influence of the non-local gradient to the pattern formation can be partially compensated with the nonlinear diffusion (Figures 6, 7 and 8). However, the non-local sampling and the nonlinear diffusion do not yield in patterns more similar to the experimentally observed ones when compared to the patterns obtained by the corresponding model with the local sampling and the linear diffusion.

The more precise and sophisticated two- and three-dimensional computational models implying the formation of structures observed on bioluminescence images are now under development and testing.

## ACKNOWLEDGMENT

The research by R. Baronas is funded by the European Social Fund under Measure VP1-3.1-ŠMM-07-K "Support to Research of Scientists and Other Researchers (Global Grant)", Project "Developing computational techniques, algorithms and tools for efficient simulation and optimization of biosensors of complex geometry".

## REFERENCES

- [1] R. Baronas, "Simulation of bacterial self-organization in circular container along contact line as detected by bioluminescence imaging," in *SIMUL 2011: The Third International Conference on Advances in System Simulation*, Barcelona, Spain, Oct. 2011, pp. 156–161.
- [2] M. Eisenbach, *Chemotaxis*. London: Imperial College Press, 2004.
- [3] T. C. Williams, *Chemotaxis: Types, Clinical Significance, and Mathematical Models*. New York: Nova Science, 2011.
- [4] J. D. Murray, *Mathematical Biology: II. Spatial Models and Biomedical Applications*, 3rd ed. Berlin: Springer, 2003.
- [5] E. F. Keller and L. A. Segel, "Model for chemotaxis," *J. Theor. Biol.*, vol. 30, no. 2, pp. 225–234, 1971.
- [6] T. Hillen and K. J. Painter, "A user's guide to PDE models for chemotaxis," *J. Math. Biol.*, vol. 58, no. 1-2, pp. 183–217, 2009.
- [7] E. O. Budrene and H. C. Berg, "Dynamics of formation of symmetrical patterns by chemotactic bacteria," *Nature*, vol. 376, no. 6535, pp. 49–53, 1995.
- [8] M. P. Brenner, L. S. Levitov, and E. O. Budrene, "Physical mechanisms for chemotactic pattern formation by bacteria," *Biophys. J.*, vol. 74, no. 4, pp. 1677–1693, 1998.
- [9] S. Sasaki *et al.*, "Spatio-temporal control of bacterial-suspension luminescence using a PDMS cell," *J. Chem. Engineer. Japan*, vol. 43, no. 11, pp. 960–965, 2010.
- [10] K. J. Painter and T. Hillen, "Spatio-temporal chaos in a chemotactic model," *Physica D*, vol. 240, no. 4-5, pp. 363–375, 2011.
- [11] R. Šimkus, "Bioluminescent monitoring of turbulent bioconvection," *Luminescence*, vol. 21, no. 2, pp. 77–80, 2006.
- [12] R. Šimkus, V. Kirejev, R. Meškienė, and R. Meškys, "Torus generated by *Escherichia coli*," *Exp. Fluids*, vol. 46, no. 2, pp. 365–369, 2009.
- [13] S. Daunert *et al.*, "Genetically engineered whole-cell sensing systems: coupling biological recognition with reporter genes," *Chem. Rev.*, vol. 100, no. 7, pp. 2705–2738, 2000.
- [14] Y. Lei, W. Chen, and A. Mulchandani, "Microbial biosensors," *Anal. Chim. Acta*, vol. 568, no. 1-2, pp. 200–210, 2006.
- [15] M. B. Gu, R. J. Mitchell, and B. C. Kim, "Whole-cell-based biosensors for environmental biomonitoring and application," *Adv. Biochem. Eng. Biotechnol.*, vol. 87, pp. 269–305, 2004.
- [16] R. Šimkus and R. Baronas, "Metabolic self-organization of bioluminescent *Escherichia coli*," *Luminescence*, vol. 26, no. 6, pp. 716–721, 2011.
- [17] R. Baronas and R. Šimkus, "Modeling the bacterial self-organization in a circular container along the contact line as detected by bioluminescence imaging," *Nonlinear Anal. Model. Control*, vol. 16, no. 3, pp. 270–282, 2011.
- [18] A. A. Samarskii, *The Theory of Difference Schemes*. New York-Basel: Marcel Dekker, 2001.
- [19] I. R. Lapidus and R. Schiller, "Model for the chemotactic response of a bacterial population," *Biophys. J.*, vol. 16, no. 7, pp. 779–789, 1976.

- [20] P. K. Maini, M. R. Myerscough, K. H. Winters, and J. D. Murray, "Bifurcating spatially heterogeneous solutions in a chemotaxis model for biological pattern generation," *Bull. Math. Biol.*, vol. 53, no. 5, pp. 701–719, 1991.
- [21] R. Tyson, S. R. Lubkin, and J. D. Murray, "Model and analysis of chemotactic bacterial patterns in a liquid medium," *J. Math. Biol.*, vol. 38, no. 4, pp. 359–375, 1999.
- [22] R. Kowalczyk, "Preventing blow-up in a chemotaxis model," *J. Math. Anal. Appl.*, vol. 305, no. 2, pp. 566–588, 2005.
- [23] M. R. Myerscough, P. K. Maini, and K. J. Painter, "Pattern formation in a generalized chemotactic model," *Bull. Math. Biol.*, vol. 60, no. 1, pp. 1–26, 1998.
- [24] E. F. Keller and L. A. Segel, "Travelling bands of chemotactic bacteria: A theoretical analysis," *J. Theor. Biol.*, vol. 30, no. 2, pp. 235–248, 1971.
- [25] K. Painter and T. Hillen, "Volume-filling and quorum-sensing in models for chemosensitive movement," *Can. Appl. Math. Quart.*, vol. 10, no. 4, pp. 501–543, 2002.
- [26] J. J. L. Velazquez, "Point dynamics for a singular limit of the Keller-Segel model. I. Motion of the concentration regions," *SIAM J. Appl. Math.*, vol. 64, no. 4, pp. 1198–1223, 2004.
- [27] H. G. Othmer and T. Hillen, "The diffusion limit of transport equations II: Chemotaxis equations," *SIAM J. Appl. Math.*, vol. 62, no. 4, pp. 1122–1250, 2002.
- [28] T. Hillen, K. Painter, and C. Schmeiser, "Global existence for chemotaxis with finite sampling radius," *Discr. Cont. Dyn. Syst. B*, vol. 7, no. 1, pp. 125–144, 2007.
- [29] R. Baronas, F. Ivanauskas, and J. Kulys, *Mathematical Modeling of Biosensors: An Introduction for Chemists and Mathematicians*, ser. Springer Series on Chemical Sensors and Biosensors, G. Urban, Ed. Dordrecht: Springer, 2010.
- [30] R. Čiegis and A. Bugajev, "Numerical approximation of one model of bacterial self-organization," *Nonlinear Anal. Model. Control*, vol. 17, no. 3, pp. 253–270, 2012.
- [31] S. Leestma and L. Nyhoff, *Pascal Programming and Problem Solving*, 4th ed. New York: Prentice Hall, 1993.
- [32] R. Tyson, L. Stern, and R. J. LeVeque, "Fractional step methods applied to a chemotaxis model," *J. Math. Biol.*, vol. 41, no. 5, pp. 455–475, 2000.
- [33] P. Romanczuk, U. Erdmann, H. Engel, and L. Schimansky-Geier, "Beyond the Keller-Segel model. Microscopic modeling of bacterial colonies with chemotaxis," *Eur. Phys. J. Special Topics*, vol. 157, no. 1, pp. 61–77, 2007.